Available online at www.sciencedirect.com
ScienceDirect
Catalysis Today 117 (2006) 484–490
CATALYSIS TODAY
www.elsevier.com/locate/cattod

Microemulsion synthesis of MgO-supported $LaMnO_3$ for catalytic combustion of methane

Erik Elm Svensson *, Stylianos Nassos, Magali Boutonnet, Sven G. Järås

KTH-Royal Institute of Technology, Chemical Technology, Teknikringen 42, SE-10044 Stockholm, Sweden

Abstract

Catalysts with 20% $LaMnO_3$ supported on MgO have been prepared via CTAB-1-butanol-*iso*-octane-nitrate salt microemulsion. The preparation method was successfully varied in order to obtain different degrees of interaction between $LaMnO_3$ and MgO as shown by TPR and activity tests after calcination at 900 °C. Activity was tested on structured catalysts with 1.5% CH_4 in air as test gas giving a GHSV of 100,000 h^{-1}. The activity was greatly enhanced by supporting $LaMnO_3$ on MgO compared with the bulk $LaMnO_3$. After calcination at 1100 °C both the surface area and TPR profiles were similar, indicating that the preparation method is of little importance at this high temperature due to interaction between the phases. Pure $LaMnO_3$ and MgO were prepared using the same microemulsion method for comparison purposes. Pure MgO showed an impressive thermal stability with a BET surface area exceeding 30 m^2/g after calcination at 1300 °C. The method used to prepare pure $LaMnO_3$ appeared not to be suitable since the surface area dropped to 1.1 m^2/g already after calcination in 900 °C.

Keywords: Catalytic combustion; Methane; $LaMnO_3$; MgO; Microemulsion

1. Introduction

Due to more stringent legislation concerning emissions of NO_X, CO and hydrocarbons during the last years, catalytic combustion has emerged as a very promising technique for gas turbine applications. Several reviews have been published in this area that clearly show the potential of the technique to achieve ultra-low levels of emissions [1–3]. The most common fuel for gas turbines is natural gas [4], which mainly consists of methane. In catalytic combustion the temperature needed for efficient combustion of natural gas can be lowered compared with flame combustion, it is therefore possible to decrease the formation of thermal NO_X.

Perovskites have been extensively studied due to their high catalytic activity in methane combustion and their ability to operate in higher temperatures than noble metals [1]. Perovskites normally show a very low surface area and even though research has yielded perovskites with high surface area in the lower temperature range, their strong tendency to sinter results in a rapid decrease of the surface area above 900 °C [5]. By supporting the perovskite on a material less prone to sintering this problem can be circumvented. The task of the support is to disperse the perovskite and prevent contact between the perovskite particles in order to avoid sintering. This has to be fulfilled without giving rise to solid-state reactions between support and perovskite, causing sintering and/or forming less active species. The most studied support γ-Al_2O_3 has shown to interact negatively with $LaMnO_3$ after calcination at 1100 °C, even if the support is first stabilised with lanthanum [5].

Magnesia (MgO) is a much more thermally stable support compared to γ-Al_2O_3. Even after such a severe calcination temperature as 1400 °C, MgO has been shown to retain a BET surface area in the range of 10 m^2/g, whereas Al_2O_3 and ZrO_2 after the same treatment show a surface area in the range of 1 m^2/g [6]. The preparation method has shown to be of major importance for the thermal stability of MgO. MgO developed by Ube Industries [7] by growing crystals in a turbulent flow of magnesium vapour and oxygen resulted in MgO that after calcination in 1500 °C had a surface area of 72 m^2/g [8], whereas MgO prepared by Berg et al. showed a surface area of less than 1 m^2/g after the same treatment [9]. Due to the basic nature of magnesia it dissolves in water with low pH. When in contact with neutral and basic aqueous solutions MgO can form $Mg(OH)_2$, which after calcination results in MgO with different

---

* Corresponding author. Tel.: +46 8 7908243; fax: +46 8 108579.
E-mail address: eelm@ket.kth.se (E.E. Svensson).

0920-5861/$ – see front matter © 2006 Elsevier B.V. All rights reserved.
doi:10.1016/j.cattod.2006.06.014

morphology than the initial one [10]. Conventional impregnation techniques with aqueous solutions will thus result in magnesium mixed with the active component with an imminent risk of forming mixed species besides changing the properties of the support. This phenomenon was also observed in a study by Cimino et al. when a water-based preparation method was utilized [5]. An interaction between the $LaMnO_3$ and MgO was observed as a change in redox behaviour compared to the bulk $LaMnO_3$. The MgO-supported $LaMnO_3$ had a substantially larger H_2-consumtion, which the author attributed to formation of Mg partially substituted perovskite forcing a large portion of Mn^{3+} into Mn^{4+} to balance the total charge. Large amounts of Mn^{4+} can increase the catalytic activity due to an increased ability of lattice oxygen close to Mn^{4+} to take part in methane oxidation [11]. Saracco et al. also observed this in a study [11], in which partial substitution of $LaMn_{1-X}Mg_XO_3$ with $X = 0–0.5$ was investigated. In the same study Saracco et al. observed an increase in activity with increased Mg-substitution up to $X = 0.2$. Further Mg-substitution resulted, however, in lower activity, which the authors explained by the possibility that Mg reduced the amount of cation vacancies present in pure $LaMnO_3$. In the same study the substituted perovskite with the same composition was also supported on MgO to a level of 25 wt% perovskite in an attempt to decrease the sintering of the perovskite. The sintering was in fact decreased substantially, but the surface area of the supported catalysts was not as high as what would be expected from MgO alone suggesting that some kind of interaction between support and perovskite was promoting sintering in the support. Another indication of this could be observed in the activity tests, where no positive effect of higher degree of Mg-substitution could be observed for the supported catalysts. The authors attributed this to the fact that the MgO was blocking access to the perovskite, which according to electron microscopy appeared to be more pronounced in the sample with the highest Mg-substitution. Another explanation could be the preparation method, where Mg, La and Mn were intimately mixed according to the citrate method described in [12]. The perovskite was thus allowed to be in equilibrium with the magnesium and high degree of Mg-substitution could have been present even in the sample with equimolar mixture of La and Mn.

The microemulsion technique has emerged as a powerful technique to control the shape and size of particles during synthesis of catalysts [13]. When using the microemulsion technique for synthesis of nano-particles, the present surfactants can control the growth of the particles and thereby make it possible to obtain particles with narrow size distribution. The microemulsion technique also offers the possibility to control the mixing of the components. Besides obtaining high degree of mixing between components, controlled separation of components can in some cases give beneficial properties to the catalyst. For example, an active component can be added to a support by first precipitating the support precursor within a microemulsion. The precursor of the active component can then be precipitated on the surface of the support. In this configuration the stability of the support can be utilized without blocking the access to the active component.

The objective of this work was to investigate the possibility to use the microemulsion technique to prepare high-surface area MgO with highly dispersed $LaMnO_3$. The preparation method was varied in an attempt to control the degree of interaction between MgO and $LaMnO_3$, in order to retain the stable properties of MgO and simultaneously obtain high dispersion of $LaMnO_3$.

2. Experimental

2.1. Catalyst preparation

For all catalyst prepared by the microemulsion method, the same composition of the microemulsion system was utilized as used by Palla et al. [14]. The composition can be found in Table 1. Magnesium nitrate ($Mg(NO_3)_2·6H_2O$) was used as MgO precursor and lanthanum nitrate ($La(NO_3)_3·6H_2O$) and manganese nitrate ($Mn(NO_3)_2·XH_2O$) were used as $LaMnO_3$ precursor. All chemicals used were supplied by Aldrich and were of reagent grade.

2.1.1. Bulk magnesia

Magnesia was prepared with a conventional aqueous method (MgO-Conv) and using the microemulsion technique (MgO-ME) by precipitating $Mg(NO_3)_2$ with ammonia. The amount of ammonia used was 1.5 times the stoichiometric amount to form $Mg(OH)_2$. In both cases the $Mg(NO_3)_2$ was dissolved in deionised water (Milli-Q). In the conventional method, the magnesium solution was slowly added to a NH_3 solution. Similarly, for the microemulsion technique the magnesium solution was used as the water phase of one microemulsion. This microemulsion was added to a second microemulsion containing an ammonia solution. In both cases the precipitated particles were aged for 24 h. After aging, the particles were recovered by means of centrifugation. In the conventional method the particles were washed first with water and then with methanol. After each wash, centrifugation was used to collect the particles. The same procedure was used for the microemulsion technique but the first wash was performed with a chloroform/methanol mixture (1:1 based on volume) instead of water in order to remove most of the surfactant. The particles were dried at 60 °C for 12 h and thereafter grinded in a mortar and divided in three crucibles. The materials were calcined for 4 h in flowing air at 900, 1100 and 1300 °C, respectively. Ramping speed was set to 2 °C/min with a slower ramping speed of 0.5 °C/min between 200 and 400 °C.

Table 1
Composition of the microemulsion system used in the study

Phase	Compound	Composition (%)
Oil	*Iso*-octane	53.9
Surfactant	CTAB (cetyl tri-methyl ammonium bromide)	13.5
Co-surfactant	1-Butanol	12.0
Water	Water Mg-, La-, Mn-nitrates, ammonia (28–30%)	20.6

2.1.2. MgO-supported $LaMnO_3$

In order to achieve different degree of interaction between the MgO and $LaMnO_3$, the method of mixing the two components in the microemulsion was varied, which is the point in the synthesis at which the perovskite precursor was introduced to the magnesia. Three preparation methods were tested (termed ME-Coprec, ME-1 and ME-2), all resulting in materials with the nominal composition of 20 wt% $LaMnO_3$ supported on MgO.

In the first method (ME-Coprec), the MgO and the $LaMnO_3$ precursors were co-precipitated by hosting a water solution of Mg-, La- and Mn-nitrate in one microemulsion and mixing it with a second microemulsion containing a 1.5 stoichiometric amount of ammonia in a similar way as the bulk MgO.

In the second method (ME-1) the Mg-nitrate was precipitated with ammonia and the La- and Mn-nitrate were precipitated on the surface of the $Mg(OH)_2$ after aging for 24 h. The $LaMnO_3$ precursor was allowed to fully react for 2 h before recovery.

In the third method (ME-2) the MgO precursor and the $LaMnO_3$ precursor were precipitated separately with ammonia and aged for 24 h, before mixing the two microemulsions and recovering the particles.

The same recovery and washing procedure as used for bulk MgO prepared by the microemulsion technique was used for the MgO-supported $LaMnO_3$.

The incipient wetness technique was used to impregnate 20 wt% of $LaMnO_3$ on MgO using bulk MgO prepared both by the conventional aqueous method (IW-Conv) and the microemulsion technique (IW-ME). The MgO used for impregnation was pre-calcined at the respective temperature of the final supported catalyst, i.e. 900 and 1100 °C. Recognising the risk of dissolving MgO and/or forming $Mg(OH)_2$ resulting in changes in the morphology, methanol was used as solvent for the $LaMnO_3$ precursor. The concentration of the La:Mn (molar ratio 1:1) in the methanol was 0.94 and 0.82 M for IW-Conv and IW-ME, respectively. Methanol has been reported not to influence MgO [10]. However, since the nitrates used as $LaMnO_3$-precursor contain crystal water, water was present in the resulting impregnation solutions. The impregnation was repeated three times with drying at 60 °C for at least 2 h in-between each impregnation.

All MgO supported $LaMnO_3$ catalysts were calcined for 4 h in flowing air at 900 or 1100 °C. Ramping speed was set to 2 °C/min with a slower ramping speed of 0.5 °C/min between 200 and 400 °C.

2.1.3. Bulk $LaMnO_3$

Bulk $LaMnO_3$ was prepared using the same microemulsion technique used for the MgO-supported $LaMnO_3$. A similar technique was successfully used by Giannakas et al. [15]. A microemulsion with a water solution of La- and Mn-nitrate was mixed with a microemulsion containing ammonia. The same recovery and washing procedure was used as for all materials prepared by the microemulsion technique. After drying at 60 °C for 12 h the powder was crushed and calcined for 4 h in flowing air at 900 and 1100 °C. Ramping speed was set to 2 °C/min with a slower ramping speed of 0.5 °C/min between 200 and 400 °C.

2.2. Characterisation

Surface area and pore size distribution were measured by nitrogen adsorption at liquid N_2 temperature using a Micromeretics ASAP 2010 instrument. The crystal phases were determined by X-ray diffraction (XRD), using a Siemens Diffraktometer D5000 scanning 2θ from 10° to 90° using monochromatised Cu Kα radiation. Crystal phases were identified using JCPDS files. Temperature programmed reduction (TPR) was performed using a Micromeretics Autochem 2910 equipped with a thermal conductivity detector (TCD). Approximately 0.2 g of bulk $LaMnO_3$ and 0.5 g of MgO-supported $LaMnO_3$ was used in the TPR analysis. After pre-treatment in 5% O_2/He at 800 °C for 30 min, the sample was reduced with 5% H_2/Ar (30 cm^3/min) heating 10 °C/min from room temperature to 900 °C. The concentration of manganese in the manganese nitrate was determined by flame-AAS using a Perkin-Elmer Model 110 OB. The same instrument was used to determine the amount of manganese in the catalyst samples.

2.3. Activity tests of supported catalysts

The supported catalysts calcined at 900 °C were tested for their catalytic activity in methane combustion. For comparison purposes, bulk $LaMnO_3$, IW-ME and IW-Conv (calcined at 900 °C) and MgO-Conv and MgO-ME (calcined at 1100 °C) were also tested. The materials were coated on monoliths (Corning, 400 cpsi) with 14 mm diameter and 10 mm length. Slurries consisting of methanol and catalyst powder (20 wt% catalyst) were prepared by ball milling for 24 h. Thereafter, the monoliths were dipped in the slurries. The excess slurry was removed by blowing compressed air through the monolith channels after which the monolith was dried in 90 °C for 0.5 h. The dipping/drying procedure was repeated until catalyst loadings of 20 wt% of the total weight (monolith and catalyst) were reached, which demanded five, six coatings for each monolith. The coated monoliths were calcined at 800 °C for 2 h.

The activity of the catalysts was tested in a tubular reactor operating in atmospheric pressure, consisting of a quartz tube inserted in an electrically heated oven. The temperature was measured a few millimetres before and after the catalyst with N-type thermocouples inserted in closed alumina-tubes. The temperature in front of the catalyst was used as the catalyst temperature. The reacting gas mixture consisted of 1.5% methane in air giving a space velocity of 100,000 h^{-1} (based on the total volume of the monolith). The temperature of the oven was ramped from 300 to 900 °C twice, using the ignition curve from the second heating ramp to compare the catalysts. The gas exiting the reactor was analysed for CH_4, CO, CO_2, O_2, H_2, NO and NO_2 in a continuous system of a series of analysers using the principle of NDIR- and UV-spectroscopy, paramagnetism and thermal conductivity.

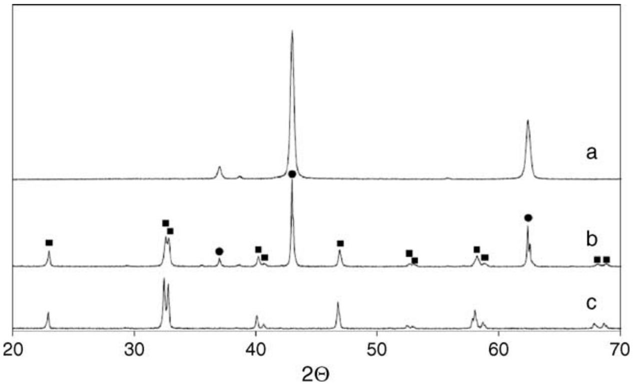

Fig. 1. Typical XRD-diffractograms for MgO (a), 20% $LaMnO_3$/MgO (b), and $LaMnO_3$ (c). Actual catalysts used were MgO-ME (a), IW-ME (b), and LaMn (c), all calcined at 1100 °C. Phases observed are marked out in sample 'b' and were MgO (●) and rhombohedral $LaMnO_3$ (■). The same phases can be identified in samples 'a' and 'c'.

3. Results and discussion

3.1. Structural properties

No other crystalline phases besides the expected MgO and $LaMnO_3$ were detected in the samples by XRD. However, the $LaMnO_3$ was in rhombohedral configuration (JCPDS 32-0484) even after calcination at 1100 °C. Saracco et al. [11] found that an orthorhombic structure replaced the rhombohedral structure after calcination at 1100 °C or above. A rhombohedral structure is preferable since it has higher catalytic activity due to higher degree of cation vacancies [11,16]. In Fig. 1, one typical X-ray diffractogram for each group of materials is presented. The three groups were bulk MgO, bulk $LaMnO_3$ and MgO-supported $LaMnO_3$. No other phases were identified for the other prepared materials within the above groups.

The X-ray diffractograms were used to determine the crystallite size of the phases. The crystallite size of $LaMnO_3$ and MgO can be found in Table 2. It was clearly observed that MgO effectively prevents crystal growth of $LaMnO_3$ since the crystallite size of the supported $LaMnO_3$ was significantly smaller compared to the unsupported $LaMnO_3$. The different preparation methods of the MgO-supported $LaMnO_3$ did result in differences in $LaMnO_3$ crystallite size. The impregnated catalysts displayed smallest crystallite sizes after calcination at 900 °C and ME-Coprec the largest. After calcination at 1100 °C it could be observed that crystal growth of $LaMnO_3$ occurred significantly less in ME-Coprec and ME-1 compared to the other materials.

Additionally, it was observed that the presence of $LaMnO_3$ induced crystal growth of MgO. While the crystallite size in bulk MgO after calcination at 900 °C was in the range of 40 nm, the supported catalysts prepared by the microemulsion method showed crystallite sizes in the range of 80–100 nm. The impregnated samples displayed smaller MgO crystallites. Increasing the calcination temperature to 1100 °C hardly changed the crystallite size in bulk MgO, while the supported catalysts displayed significant crystal growth.

Major differences in the surface area (BET) could be observed for the materials as seen in Table 2. Bulk $LaMnO_3$ showed major sintering. Already after calcination in 900 °C the surface area was 1.1 m^2/g and after calcination in 1100 °C a very low surface area of 0.5 m^2/g was detected. On the other hand, both preparation methods of bulk MgO exhibited an impressive thermal stability. The surface area exhibited by both MgO-ME and MgO-Conv greatly surpasses the surface area obtained in the study by Berg et al. [9]. For this reason the preparation of both materials was repeated and calcined at 1100 and 1300 °C. It was shown that both MgO-materials were reproducible since the surface area was practically identical with the previously prepared materials. The surface area of MgO-Conv was initially (at 900 °C) higher but when increasing the calcination temperature, MgO-ME retains the surface area better. An explanation of this could be found from the pore-size distribution (Fig. 2) where it could be observed that the MgO-Conv contains a larger portion of micro-pores compared to MgO-ME. Micro-pores are known to have a larger tendency to collapse in high temperature compared to meso-pores [17]. Furthermore, in catalytic combustion micro-pores could complicate the access to the catalyst surface when very high space velocities are used [17]. The same stability exhibited by bulk MgO was not obtained for any of the supported catalysts. When observing the surface areas after calcination in 900 °C, a trend can be seen: surface area decreased in the order ME-2 > ME-1 > ME-Coprec, which indicates that a closer contact between $LaMnO_3$ and MgO decreases the stability. In order to

Table 2
Catalyst identification code with respective nominal composition

Catalyst ID	Nominal composition	BET surface area (m^2/g)			Crystallite size determined by XRD (nm)			
					$LaMnO_3$		MgO	
		900 °C	1100 °C	1300 °C	900 °C	1100 °C	900 °C	1100 °C
LaMn	$LaMnO_3$	1.1	0.5	–	145	162	–	–
MgO-ME	MgO	56.3	42.5	35.4	–	–	46	49
MgO-Conv	MgO	65.2	46.6	34.5	–	–	41	46
ME-Coprec	20% $LaMnO_3$/MgO	7.1	1.2	–	57	88	82	143
ME-1	20% $LaMnO_3$/MgO	9.8	1.7	–	52	83	98	128
ME-2	20% $LaMnO_3$/MgO	11.5	2.0	–	53	102	85	130
IW-ME	20% $LaMnO_3$/MgO	7.5	2.0	–	47	96	68	124
IW-Conv	20% $LaMnO_3$/MgO	8.7	2.5	–	48	94	73	119

BET surface area and crystallite size of $LaMnO_3$ and MgO determined with XRD were measured after calcination in flowing air for 4 h in respective temperature.

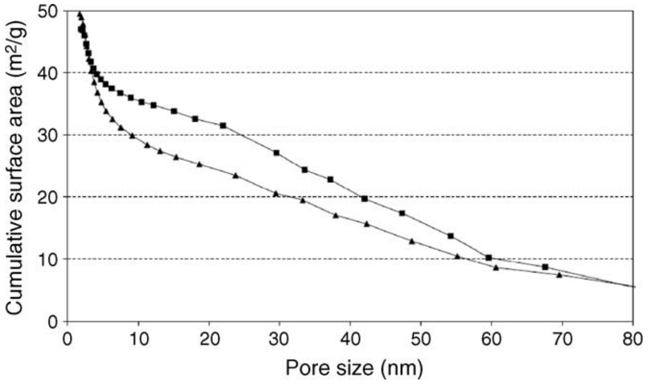

Fig. 2. Pore size distribution with the cumulative surface area with pore size for MgO-Conv (▲) and MgO-ME (■). Both samples were calcined at 1100 °C for 4 h in air.

verify that this was not a coincidence, the preparations of these samples were repeated. The results were shown to be reproducible and the same trend was again observed. This trend could also be seen for the materials calcined at 1100 °C, but at these low surface area values, the BET-measurement cannot be considered reliable. Impregnation with $LaMnO_3$ after calcining MgO (IW-ME and IW-Conv) could not stop the negative effect of the perovskite on the stability of the support. Already after calcination at 900 °C the surface area dropped from around 60 m^2/g before impregnation to less than 10 m^2/g, which to some extent could be explained by pores blocked by the perovskite. The influence of the $LaMnO_3$ was further observed after calcination at 1100 °C when the surface area dropped significantly even if these catalysts retained the highest surface area of the supported catalysts. Another explanation of the drop in surface area after impregnation of IW-ME and IW-Conv could be that the water present in the impregnation solutions caused formation of $Mg(OH)_2$. As mentioned in the introduction this process can change the morphology of the MgO. This explanation might be the most likely since the redox-properties of the impregnated samples suggested that the interaction between $LaMnO_3$ and MgO was lower compared to the other catalysts. This will be further discussed in Section 3.2.

3.2. Redox-properties

The TPR profiles of the supported catalysts after calcination at 900 and 1100 °C can be found in Fig. 3a–d, respectively. The catalysts are compared with the bulk $LaMnO_3$ and ME-Coprec calcined at the corresponding temperature. Bulk $LaMnO_3$ gives rise to two main peaks: the first with a maximum at approximately 460–470 °C and a second at the maximum temperature of the analysis, which was 900 °C. The first peak in the literature has been attributed to reduction of Mn^{4+} to Mn^{3+} and the second to reduction of Mn^{3+} to Mn^{2+} [18]. The first peak is thus an indication of the oxygen excess (δ) in the perovskite

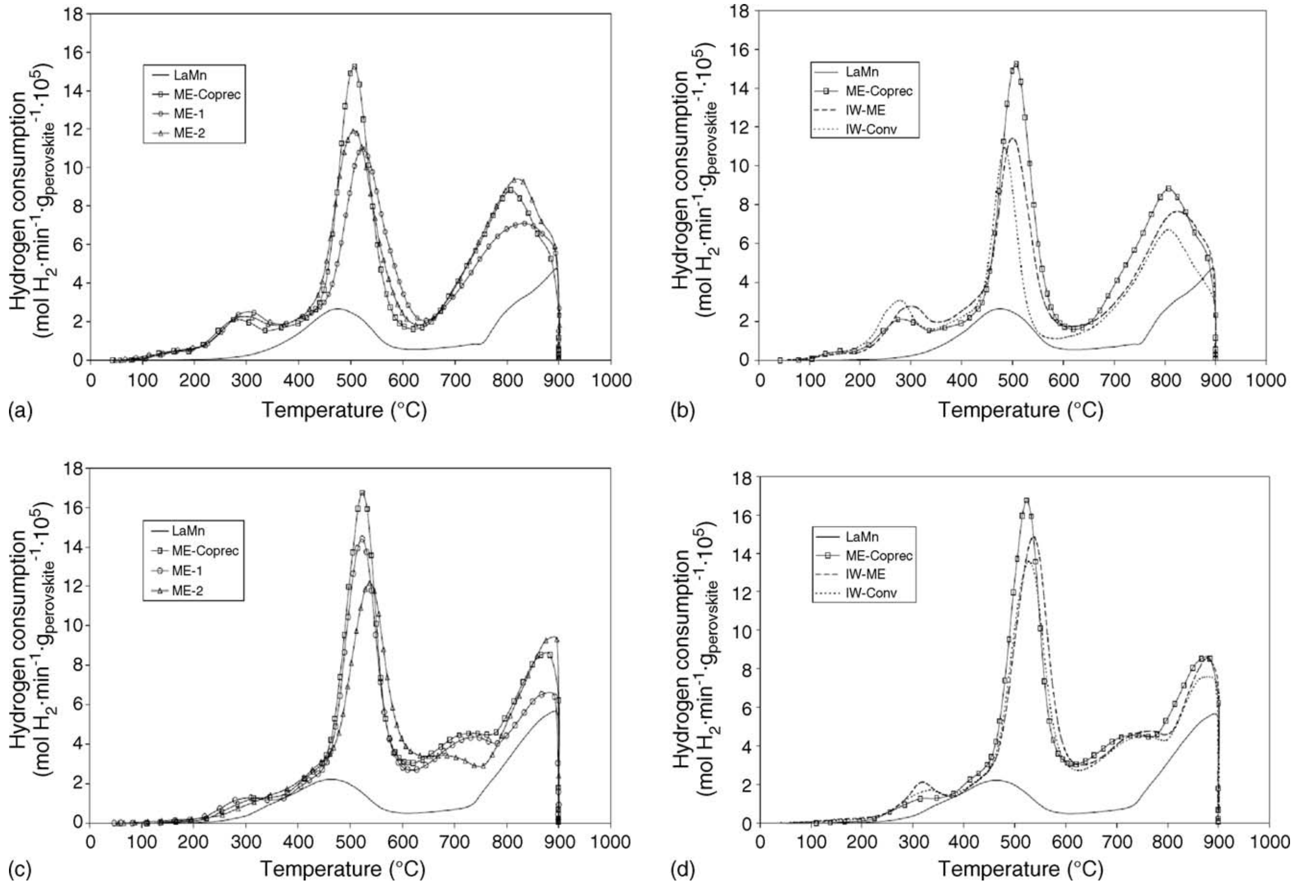

Fig. 3. TPR profiles of the supported catalysts compared with unsupported $LaMnO_3$. For comparison purposes ME-Coprec can be found in all profiles. Catalysts were calcined at: (a and b) 900 °C and (c and d) at 1100 °C.

Table 3
Hydrogen consumption measured for the catalysts containing $LaMnO_3$

Catalyst	First step (<600 °C) H_2 consumption (mol H_2/mol Mn)		Total (900 °C) H_2-consumption (mol H_2/mol Mn)	
	900 °C	1100 °C	900 °C	1100 °C
LaMn	0.11	0.11	0.50	0.52
ME-Coprec	0.43	0.41	0.89	0.88
ME-1	0.41	0.38	0.88	0.82
ME-2	0.40	0.37	0.87	0.84
IW-ME	0.39	0.42	0.80	0.91
IW-Conv	0.33	0.38	0.65	0.83

Hydrogen consumption is expressed in mol hydrogen consumed/mol manganese present in the sample.

and is highly related to the catalytic activity. Reduction of manganese to Mn^{2+} in the second peak means that MnO and La_2O_3 are formed and that there is a loss of the perovskite structure. This process is not likely to be finished yet at 900 °C. This is also confirmed by the total H_2-consumption, which is not large enough to reduce all of the manganese to Mn^{2+} (Table 3). Table 3 is divided in H_2-consumption for the first step (up to 600 °C) and the total H_2-consumption and displays all values obtained for the materials containing perovskite. The H_2-consumption below 600 °C will give an indication of the amount of Mn^{4+} in the material, which for the supported catalyst could be linked to the degree of Mg-substitution in the $LaMnO_3$ [11]. As seen in Table 3, the supported catalysts have a substantially higher H_2-consumption compared with the bulk $LaMnO_3$, especially in the first step. After calcination at 900 °C, all the supported catalysts exhibit an additional peak at temperature 280–300 °C, which is not present in bulk $LaMnO_3$. This is especially clear in the impregnated samples (Fig. 3b) and ME-1 (Fig. 3a). After calcination at 1100 °C this peak decreases but is still the highest in IW-ME, IW-Conv and ME-1. All these materials are expected to have the perovskite concentrated to the surface of the support and the peak might therefore be originated from Mg-substituted perovskite species with different properties at the surface. Another explanation could be segregated manganese oxide (MnO_2), which is reported to have a peak in this temperature [19]. Cimino et al. [5] observed after calcination of MgO-supported $LaMnO_3$ at 1100 °C that the main H_2-consumption peak is shifted to a higher temperature compared with bulk $LaMnO_3$. The same observation was made in this study, but already after calcination at 900 °C. The only exception was IW-Conv (to some extent also IW-ME). IW-Conv also showed a much lower H_2-consumption compared with the other supported catalysts, which indicates that the interaction between MgO and $LaMnO_3$ was less in these samples. This might also be indicated by the smaller crystallite size of MgO (Table 2) in these samples compared to the other supported catalysts. After calcination at 1100 °C the major peak is shifted in IW-ME and IW-Conv in a similar way with the other supported catalysts. The H_2-consumption also increases for these catalysts at the higher calcination temperature, which might indicate that interaction between MgO and $LaMnO_3$ occurs when the calcination temperature is increased. It can be observed that the H_2-consumption pattern is very similar for all the supported catalysts after calcination at 1100 °C, i.e. influence of the preparation method is not retained after calcination in 1100 °C.

3.3. Combustion activity

Catalytic activity was measured on catalytic materials supported on cordierite monoliths. The result from the activity test can be found in Fig. 4. For all catalyst with $LaMnO_3$ supported on MgO, the only detected product from oxidation of CH_4 was CO_2. For the two MgO samples (MgO-ME and MgO-Conv), on the other hand, large amounts of CO and H_2 were detected. Not until the temperature approached 900 °C was CO_2 the only detected product, resembling the result obtained by Berg et al. [9]. It can also be observed that MgO-ME is slightly more active compared to MgO-Conv in temperatures above 725 °C. This might be explained by the larger amount of large pores for the MgO-ME (Fig. 2), which can reduce mass-transfer limitations that often are observed in these high temperatures.

The beneficial effect in terms of activity by depositing $LaMnO_3$ on MgO compared with using unsupported $LaMnO_3$ can clearly be observed in Fig. 4. All catalysts prepared by depositing $LaMnO_3$ with the microemulsion technique have higher activity than catalysts with perovskite impregnated with the incipient wetness technique. This might be due to less Mg-substitution in the perovskite of the impregnated catalysts as indicated by TPR and MgO crystallite size. Another explanation could be the dramatic drop in surface area after calcination causing pore closure and consequently encapsulation of perovskite inside the support. The different supports used for impregnation showed no effect since the ignition curves of IW-ME and IW-Conv practically coincide.

The most active catalyst is clearly ME-1, i.e. the catalyst with $LaMnO_3$ on the surface of MgO. A probable explanation for this is that the $LaMnO_3$ is concentrated to the surface and not blocked by MgO, as observed by Saracco et al. [11]. In the study by Saracco et al. all components were co-precipitated as the material ME-Coprec prepared in this study. ME-Coprec had almost identical activity as ME-2. The different properties of

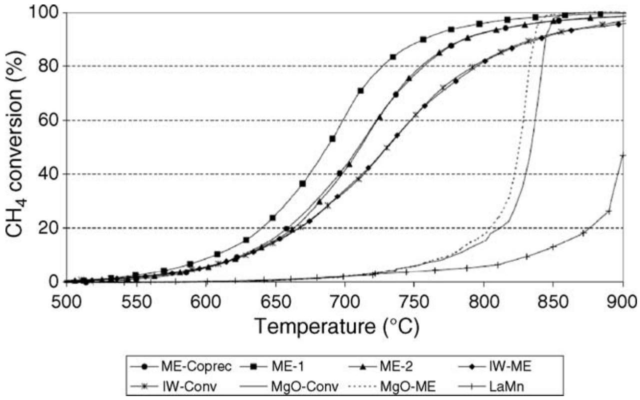

Fig. 4. Methane conversion over catalyst materials supported on cordierite monoliths. Gas composition: 1.5% CH_4 in air. GHSV = 100,000 h^{-1}.

these materials, which might increase or decrease the activity, result thus in equal activity. Firstly, the higher surface area for ME-2 might give a higher activity if the reaction is mass-transfer limited. Secondly, MgO blocking access to the perovskite as mentioned above could be a factor for both samples. The homogenous mixing of $LaMnO_3$ and MgO in ME-Coprec compared to ME-2 could make this effect more pronounced in ME-Coprec. Thirdly, higher degree of interaction between $LaMnO_3$ and MgO observed in ME-Coprec by TPR (Table 3) might both be negative and positive for the activity as previously discussed. Another explanation could also be found from the preparation method, where much larger perovskite particles were expected to form in ME-2 initially. This difference is not reflected in the crystallite size of $LaMnO_3$ (rather the opposite), but it is important to note that the crystallite size does not necessarily reflect the actual particle size.

4. Conclusions

Catalyst with 20% $LaMnO_3$ supported on MgO had been prepared by using the microemulsion technique. By varying the synthesis procedure, an attempt to vary the interaction between $LaMnO_3$ and MgO was made. Three different synthesis procedures were tested, namely:

1. Co-precipitation of both the MgO and $LaMnO_3$ (ME-Coprec).
2. Surface precipitation of the $LaMnO_3$ precursor on an aged MgO precursor (ME-1).
3. Separate precipitation of the $LaMnO_3$ and the MgO precursor, which after aging were mixed (ME-2).

Conventional techniques of preparing MgO and supported catalysts were also made for comparison purposes. Results from activity tests, TPR and surface area measurements indicate that the different preparation procedures are reflected on the properties of the material after calcination at 900 °C, probably due to variations in interaction between $LaMnO_3$ and MgO. A weak trend could be observed that segregation of the phases result in higher stability in terms of preserved surface area. The activity of the $LaMnO_3$ was greatly improved by supporting it on MgO compared with the bulk $LaMnO_3$. Highest activity was obtained over ME-1, which had the perovskite deposited on the surface of the support. After calcination at 1100 °C, however, the materials exhibit very similar properties according to TPR and surface area measurements, probably due to further interaction between the $LaMnO_3$ and MgO in this high calcination temperature.

Acknowledgement

The authors wish to acknowledge the European Union for funding through the CATHLEAN project, contract no.: ENK5-CT-2002–00683.

References

[1] M.F.M. Zwinkels, S.G. Järås, P.G. Menon, T.A. Griffin, Catal. Rev. Sci. Eng. 26 (1993) 319.
[2] L.D. Pfefferle, W.C. Pfefferle, Catal. Rev. Sci. Eng. 29 (1987) 219.
[3] P. Forzatti, Catal. Today 83 (2003) 3.
[4] R. Carroni, V. Schmidt, T. Griffin, Catal. Today 75 (2002) 287.
[5] S. Cimino, L. Lisi, R. Pirone, G. Russo, M. Turco, Catal. Today 59 (2000) 19.
[6] H. Arai, M. Machida, Appl. Catal. A: Gen. 138 (1996) 161–176.
[7] H. Arai, T. Yamada, K. Eguchi, T. Seiyama, Appl. Catal. 26 (1986) 265.
[8] I. Matsuura, Y. Hashimoto, E. Takahayasu, K. Nitta, Y. Yoshida, Appl. Catal. 74 (1991) 273.
[9] M. Berg, S.G. Järås, Catal. Today 26 (1995) 223.
[10] M. Zdrazil, Catal. Today 86 (2003) 151.
[11] G. Saracco, F. Geobaldo, G. Baldi, Appl. Catal. B: Environ. 20 (1999) 277.
[12] G. Saracco, G. Scibilia, A. Iannibello, G. Baldi, Appl. Catal. B: Environ. 8 (1996) 229.
[13] S. Eriksson, U. Nylén, S. Rojas, M. Boutonnet, Appl. Catal. A: Gen. 265 (2004) 207.
[14] B.J. Palla, D.O. Shah, P. Garcia-Casillas, J. Matutes-Aquino, J. Nanopart. Res. 1 (1999) 215.
[15] A.E. Giannakas, T.C. Vaimakis, A.K. Ladavos, P.N. Trikalitis, P.J. Pomonis, J. Colloid Interface Sci. 259 (2003) 244.
[16] J. Töpfer, J.B. Goodenough, J. Solid State Chem. 130 (1997) 117.
[17] A.J. Zarur, H.H. Whu, J.Y. Ying, Langmuir 16 (2000) 3042.
[18] L. Lisi, G. Bagnasco, P. Ciambelli, S. De Rossi, P. Porta, G. Russo, M. Turco, J. Solid State Chem. 146 (1999) 176.
[19] S. Cimino, S. Colonna, S. De Rossi, M. Faticanti, L. Lisi, J. Pettiti, P. Porta, J Catal. 205 (2002) 309.